ISBN: 978-3-95450-204-2 ISSN: 2673-5350 doi:10.18429/JACoW-IBIC2019-TUPP013

SLIT-BASED SLICE EMITTANCE MEASUREMENTS OPTIMIZATION AT PITZ

R. Niemczyk*, P. Boonpornprasert, Y. Chen, J. Good, M. Gross, H. Huck†, I. Isaev, C. Koschitzki, M. Krasilnikov, S. Lal, X. Li, O. Lishilin, G. Loisch, D. Melkumyan, A. Oppelt, H. Qian, H. Shaker, G. Shu, F. Stephan, G. Vashchenko, DESY, 15738 Zeuthen, Germany
W. Hillert, University of Hamburg, 22761 Hamburg, Germany

Abstract

At the Photo Injector Test Facility at DESY in Zeuthen (PITZ) high-brightness electron sources are optimized for use at the X-ray free-electron lasers FLASH and European XFEL. Transverse projected emittance measurements are carried out by a single-slit scan technique in order to suppress space charge effects at an energy of ~20 MeV. Previous slice emittance measurements, which employed the emittance measurement in conjunction with a transverse deflecting structure, suffer from limited time resolution and low signal-to-noise ratio (SNR) due to a long drift space from the mask to the observation screen. Recent experimental studies at PITZ show improvement of the temporal resolution and SNR by utilizing quadrupole magnets between the mask and the screen. The measurement setup is described and first results are shown.

INTRODUCTION

Low transverse emittance is crucial for high-gain x-ray free-electron lasers (FEL) [1]. During the lasing process, the radiation is amplified by the electron beam within the cooperation length, which is often much smaller than the total bunch length. The transverse emittance inside this short longitudinal slice of the electron beam, i.e., the slice emittance, is more relevant for the FEL process than the projected emittance, thus of great interest for the FEL tuning [2].

At the Photo Injector Test Facility at DESY in Zeuthen (PITZ), see Fig. 1, RF electron guns are optimized and conditioned for use at the free-electron lasers FLASH and European XFEL in Hamburg [3]. Until now, the PITZ injector was experimentally optimized based on transverse projected emittance, as a reliable slice emittance diagnostics is still not established. Since the projected emittance optimization may not coincide with slice emittance optimization [4], the slice emittance diagnostics is in preparation.

For high-energy beams, where the space charge effect is negligible, the transverse emittance is usually measured with a quadrupole scan, where the emittance is reconstructed from beam images measured after propagation through different beam optics [5]. For a correct reconstruction the beam transport matrix has to be well-known.

At PITZ low beam energies of ~20 MeV and high bunch charges on the order of 1 nC complicate the beam transport due to strong space charge effects [6]. Therefore a single-slit mask is moved through the electron beam, allowing reconstruction of the phase space from the beamlet images on a screen downstream [7–9]. From the phase space the normalized transverse emittance

$$\epsilon_{n,x} = \beta\gamma\sqrt{\langle x^2\rangle\langle x'^2\rangle - \langle xx'\rangle^2}, \quad (1)$$

is calculated, where β is the mean electron velocity normalized to the speed of light, γ the average Lorentz factor and $\langle x^2\rangle$, $\langle x'^2\rangle$ and $\langle xx'\rangle$ the second-order beam moments [3].

Placing a transverse deflecting structure (TDS) downstream the slit mask, or operating an accelerating cavity off-crest while observing the beam image in a dispersive section allows for slice emittance measurements. Time-resolved emittance measurements with the booster are limited to ~2 ps [10], while slice emittance measurements with the TDS have already reached a resolution of down to ~1 ps [11].

However, the signal strength on the screen is low due to the small number of electrons passing the slit and the long drift length. Moreover, the TDS expands the beamlet in the vertical plane, leading to a low signal-to-noise ration (SNR) which will underestimate the slice emittance due to signal removal during image noise subtraction. The use of quadrupole magnets between the slit mask and the observation screen reduces both the horizontal and vertical beta function at the measurement screen, which not only improves the time resolution, but also enhances the SNR for slice emittance measurements.

MEASUREMENT SET-UP

The RF electron gun operating at 1.3 GHz accelerates the electrons to an energy of ~6.3 MeV. A photocathode UV

* raffael.niemczyk@desy.de
† now at HZB

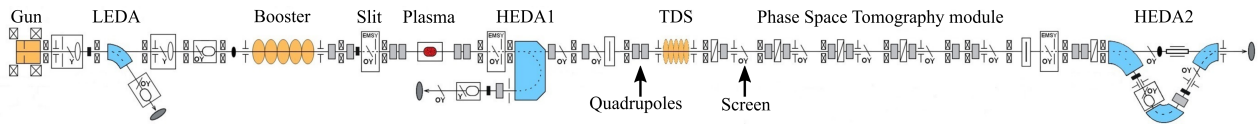

Figure 1: Schematic of the PITZ beamline.

ISBN: 978-3-95450-204-2 ISSN: 2673-5350 doi:10.18429/JACoW-IBIC2019-TUPP013

Table 1: Longitudinal position of devices at the PITZ beamline.

Element	Long. Position (m)
Cathode surface	0
Horizontal corrector dipole	4.895
Slit station EMSY1	5.277
Quadrupole magnet High1.Q09	10.208
Quadrupole magnet High1.Q10	10.388
TDS center	10.985
Observation screen	12.278

laser is used to emit electrons from a Cs_2Te cathode inside the gun. The size of the laser spot is changed with an iris in the laser beamline, which is imaged onto the photocathode. A solenoid magnet is used to focus the electron beam and compensate the emittance growth [12].

Up to 600 bunches with 1 µs separation can be accelerated at a repetition rate of 10 Hz. The beam is further accelerated in the booster (CDS) to ~20 MeV. Two slit stations (EMSY) are located between the booster and the transverse deflecting structure (TDS), both are equipped with a 10 µm-wide and a 50 µm-wide slit in both planes, allowing projected emittance measurements. A minimal projected emittance of 0.7 µm for electron bunches with 1 nC has been measured [3]. The TDS was developed in collaboration with the Institute for Nuclear Research (INR RAS, Moscow, Russia) [13]. It deflects particles in the vertical plane, allowing only for horizontal slice emittance measurements. The PITZ beamline is also equipped with three dipole spectrometers. The position of several elements in the PITZ beamline is given in Table 1. Since the lowest emittance is measured at the first EMSY station, it is of interest to measure the slice emittance at this point.

The mean beam position and average angle at a point s_2 in the beamline is expressed via the transport matrix $\mathbf{R}$ via

$$\begin{pmatrix} x_2 \\ x_2' \end{pmatrix} = \begin{pmatrix} R_{11} & R_{12} \\ R_{21} & R_{22} \end{pmatrix} \cdot \begin{pmatrix} x_1 \\ x_1' \end{pmatrix}, \quad (2)$$

where x is the transverse coordinate of the electron beam and x' the beam angle wrt the design orbit. During emittance measurements with a slit mask the angular distribution at the slit mask, i.e., s_1, is calculated from the spatial distribution at s_2 via

$$x_1' = \frac{x_2 - R_{11}x_1}{R_{12}}. \quad (3)$$

When the beam lattice from the slit mask to the observation screen is a pure drift space R_{11} becomes one and R_{12} is given by the drift length.

At PITZ, the distance from the first EMSY station to the first observation screen behind the TDS is 7.0 m. The two quadrupole magnets High1.Q09 and High1.Q10, before the TDS are used to reduce the horizontal spread of the beam on the screen by reducing R_{12} in Eq. (2), see Fig. 2. The

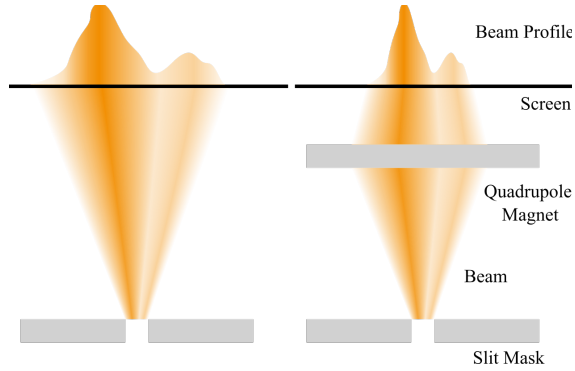

Figure 2: Scheme of an emittance measurement using a pure drift space from slit mask to the screen (left) and using quadrupole magnets behind the slit mask (right).

two quadrupole magnets behind the slit mask also focus the beam better in the vertical plane than quadrupole magnets before the slit mask due to the shorter distance between the quadrupole magnets and the observation screen.

Determination of Beam Transport Matrix

Precise knowledge of the beam transport matrix elements R_{11} and R_{12} is crucial for a correct phase space reconstruction and emittance calculation, see Eq. (3). Trajectroy response measurements are used to do an online calibration of R_{12}. For this, a horizontal corrector magnet directly in front of the first EMSY station is used. The electron beam is steered in a series of corrector settings while the quadrupole magnets are set. The beam position on the observation screen and the steering at the corrector magnet have a linear dependence propotional to R_{12}, see Eq. (2).

However, this is just the matrix element R'_{12} from the center of the corrector magnet to the observation screen. In order to calculate R_{11} and R_{12} from the slit to the observation screen, a thin-lens model is assumed . The focusing strength of the thin lens is calculated based on R'_{12}, and then R_{11} and R_{12} from the slit to the screen are calculated based on the thin-lens model.

Photoinjector Settings

For the presented slice emittance measurement the photocathode laser had a temporal flat-top profile of 17.9 ps FWHM and a transverse cylindrical profile with a diameter of 1.0 mm on the cathode. The solenoid magnet was set to 370 A for the 250 pC beam. The beam left the electron gun with a momentum of 6.3 MeV/c and was further accelerated to 19.8 MeV/c through the booster.

The slice emittance measurement has been carried out with and without any quadrupole magnets for comparison. When the quadrupole magnets were set the transport matrix elements were $R_{11} = 0.68$ and $R_{12} = 5.40$ m. The bunch length measurement with the TDS revealed a bunch length of (16.5 ± 0.1) ps with a time resolution of ~1 ps. For the slice emittance measurements, the 50 µm-wide slit was used in steps of 100 µm. In total, twenty different slit posi-

ISBN: 978-3-95450-204-2 ISSN: 2673-5350 doi:10.18429/JACoW-IBIC2019-TUPP013

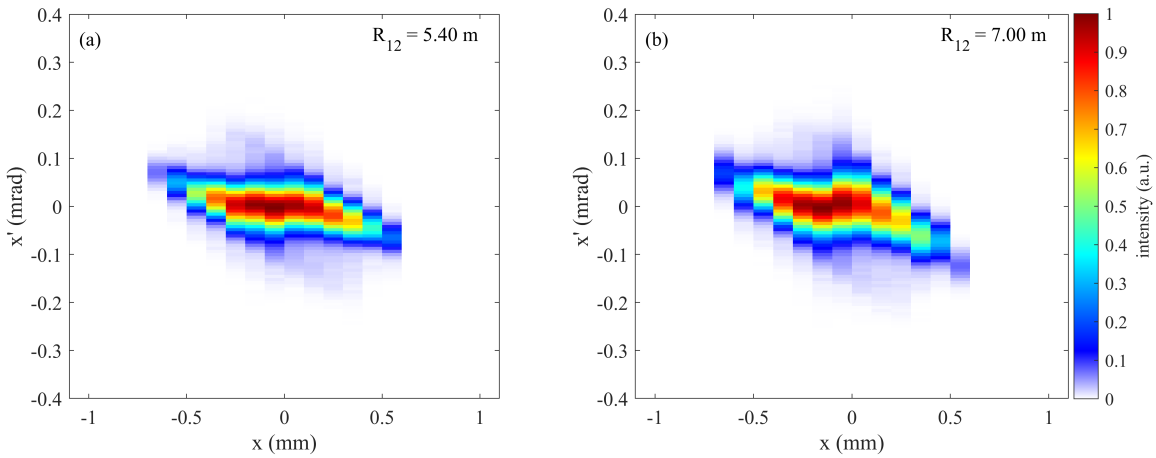

Figure 3: Phase space of the center slice, measured with (a) and without (b) the use of the quadrupole magnets High1.Q09 and High1.Q10. The emittance and the Twiss parameters of the phase space (a) are $\epsilon_x = 0.48\,\mu\text{m}$, $\alpha_x = 0.53$ and $\beta_x = 5.62\,\text{m}$, while being $\epsilon_x = 0.43\,\mu\text{m}$, $\alpha_x = 0.57$ and $\beta_x = 6.11\,\text{m}$ for phase space (b). The statistical errors are below 1%. The colorbar was kept between 0 and the maximum value in each phase space.

tions were used to reconstruct the phase space and at each slit position ten images have been taken to calculate the statistical uncertainty.

RESULTS

The phase space of the center slice, measured with the use of the quadrupole magnets High1.Q09 and High1.Q10 behind the slit and without quadrupole magnets, is shown in Fig. 3. Both phase spaces look similar, indicating that the thin-lens model is well-suited to describe the beam transport.

The slice emittances for both measurement settings, as well as the temporal bunch profile, are shown in Fig. 4. The slice emittance measured with using of the quadrupole magnets is systematically higher than the emittances measured without additional focusing. The growth in emittance by ~10% comes from a growth in the second-order beam moments. For the phase space measured with the quadrupole magnets these are $\langle x^2 \rangle = 0.0965\,\text{mm}^2$ and $\langle x'^2 \rangle = 0.0005\,\text{mrad}^2$, while being $\langle x^2 \rangle = 0.0914\,\text{mm}^2$ and $\langle x'^2 \rangle = 0.0004\,\text{mrad}^2$ for the phase space measured without quadrupole magnets. This might be due to the higher SNR, which helps during image processing to get closer to the 100% emittance.

The horizontal profile of the phase spaces can be compared with the beam profiles at the slit mask, see Fig. 5. The horizontal profile of the projected phase space, measured with use of the quadrupole magnets High1.Q09 and High1.Q10 (top) is very close to the horizontal beam profile at the slit mask, while the spacial phase space profile measured without quadrupole magnets (bottom) is narrower than the beam profile at the slit mask, indicating signal loss during image analysis. Since the beam is focused stronger, the SNR is higher and a higher fraction of the total electron

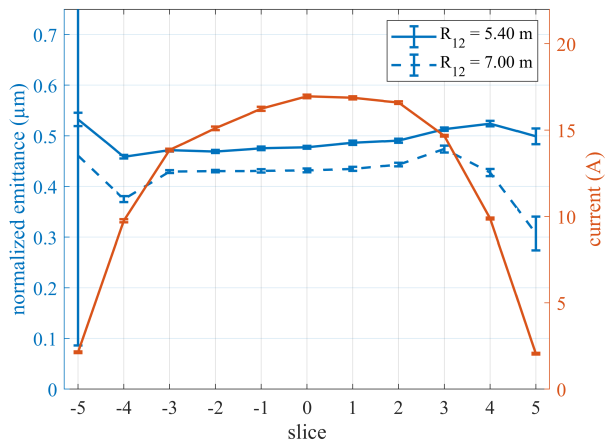

Figure 4: Measured slice emittance with (solid blue line) and without (dashed blue line) use of quadrupole magnets, temporal bunch profile (orange).

beam is measured. Besides a higher SNR, drifts in machine parameters can cause the change in emittance.

CONCLUSION

The paper shows a comparison of slice emittance measurements based on the slit scan method, with different accelerator optics. Measurements with quadrupole magnets High1.Q09 and High1.Q10 after the slit reduces R_{12} from the slit to the observation screen. The reduction of the horizontal and vertical beam size at the observation screen increases the temporal resolution and the SNR of the image, so that the measured emittance is closer to 100% emittance and shows a systematically higher slice emittance. Improved focusing in the streak direction allows reduction of

ISBN: 978-3-95450-204-2 ISSN: 2673-5350 doi:10.18429/JACoW-IBIC2019-TUPP013

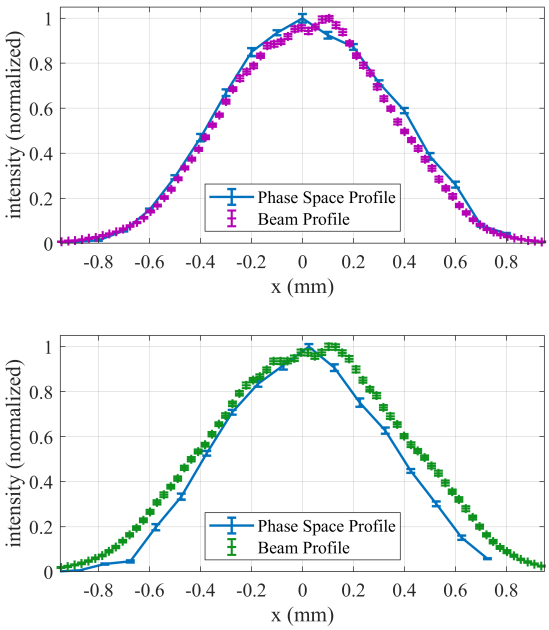

Figure 5: Horizontal profile of the projected phase space measured with quadrupole magnets and the horizontal beam profile (top) and without use of quadrupole magnets (bottom). Due to machine drifts the beam size is slightly wider in the top case (purple).

the streaking strength yielding a higher SNR while keeping the time resolution.

Measurements with different quadrupole focusing are planned in order to investigate possible systematic errors of the method. After the optimum accelerator optics for the slice emittance measurements has been found, systematic slice emittance studies can be carried out.

REFERENCES

[1] E. J. Jaeschke *et al.*, "Synchrotron Light Sources and Free-Electron Lasers", Springer Reference, p. 155, 2016.

[2] M. Yan, "Online diagnostics of time-resolved electron beam properties with femtosecond resolution for X-ray FELs", dissertation, Universität Hamburg, Germany, 2015.

[3] M. Krasilnikov *et al.*, "Experimentally minimized beam emittance from an L-band photoinjector", *Phys. Rev. ST Accel. Beams*, vol. 15, p. 100701, 2012.

[4] H. Huck *et al.*, "Progress on the PITZ TDS", in *Proc. 5th Int. Beam Instrumentation Conf. (IBIC'16)*, Barcelona, Spain, Sep. 2016, pp. 744–747. doi:10.18429/JACoW-IBIC2016-WEPG47

[5] K. McDonald and D. Russel, "Methods of emittance measurement", in *Frontiers of Particle Beams; Observation, Diagnosis and Correction*, M. Month and S. Turner, Ed. Berlin, Heidelberg: Springer Berlin Heidelberg, 1989. doi:10.1007/BFb0018284

[6] G. Kourkafas, "Incorporating space charge in the transverse phase-space matching and tomography at PITZ", dissertation, Universität Hamburg, Germany, 2015.

[7] V. Miltchev, "Investigations on the transverse phase space at a photo injector for minimized emittance", dissertation, Humboldt-Universität zu Berlin, Germany, 2006.

[8] L. Staykov, "Characterization of the transverse phase space at the photo-injector test facility in DESY, Zeuthen site", dissertation, Universität Hamburg, Germany, 2008.

[9] G. Vashchenko, "Transverse phase space studies with the new CDS booster cavity at PITZ", dissertation, Universität Hamburg, Germany, 2013.

[10] Y. Ivanisenko, "Investigation of Slice Emittance Using an Energy-chirped Electron Beam in a Dispersive Section for Photo Injector Characterization at PITZ", dissertation, Universität Hamburg, Germany, 2012.

[11] R. Niemczyk *et al.*, "Proof-of-Principle Tests for Slit-scan-based Slice Emittance Measurements at PITZ", in *Proc. 29th Linear Accelerator Conf. (LINAC'18)*, Beijing, China, Sep. 2018, pp. 553–556. doi:10.18429/JACoW-LINAC2018-TUPO098

[12] K. Floettmann, "Emittance compensation in split photoinjectors", *Phys. Rev. Accel. Beams*, vol. 20, p. 013401, 2017.

[13] L. V. Kravchuk *et al.*, "Layout of the PITZ Transverse Deflecting System for Longitudinal Phase Space and Slice Emittance Measurements", in *Proc. 25th Linear Accelerator Conf. (LINAC'10)*, Tsukuba, Japan, Sep. 2010, paper TUP011, pp. 416–418.